RSC Advances

ROYAL SOCIETY OF CHEMISTRY

www.rsc.org/advances

Cite this: DOI: 10.1039/c0xx00000x

www.rsc.org/xxxxxx

ARTICLE TYPE

Synthesis and Characterization of Well-defined PAA-PEG Multi-responsive Hydrogels by ATRP and Click Chemistry

Chao Zhou,[a] Shan-shan Qian,[a] Xia-jun Li,[b] Fang Yao,[a] John S. Forsythe*[c] and Guo-dong Fu*[a]

Received (in XXX, XXX) Xth XXXXXXXXX 20XX, Accepted Xth XXXXXXXXX 20XX

DOI: 10.1039/b000000x

Multi-responsive poly(acrylic acid)-poly(ethylene glycol) (PAA-PEG) hydrogels with well-defined crosslinking structure were synthesized using atom transfer radical polymerization (ATRP) and copper-catalyzed 1, 3-dipolar azide-alkyne cycloaddition (CuAAC) techniques. The well-defined PAA-PEG hydrogels with different degrees of crosslinking were produced from controlling the molecular weight of PAA and PEG chains. The prepared multi-responsive hydrogels exhibit regular physical and mechanical properties by adjusting the pH and Ca^{2+} ion secondary crosslinking. With increasing pH, the swelling ratio of the well-defined multi-responsive PAA-PEG hydrogels increased remarkably. Furthermore, the well-defined PAA-PEG hydrogels with Ca^{2+} secondary crosslinking possessed significantly higher crosslinking density as reflected by the lower swelling ratio, higher storage modulus, higher electrical conductivity and thermal stability. *In vitro* cell viability assay also indicates that well-defined multi-responsive PAA-PEG hydrogels are biocompatible and has potential for implantable biomaterials.

Introduction

In modern artificial organ technologies, intelligent materials are useful for controlling ion absorption and delivering a variety of therapeutic molecules such as vitamins, drugs, proteins, and minerals. These intelligent materials can be either implanted in biological tissue or replace necrotic organs.[1-3] Intelligent materials such as stimuli-responsive hydrogels, which have three-dimensional architectures and are composed of hydrophilic polymers that can absorb and retain a significant number of water, have been developed.[4, 5] The reversible volumes can be sensitive to external environmental changes that are likely to occur in biological systems such as pH,[6, 7] temperature,[8, 9] solvent composition,[10, 11] salt concentration,[12] and electric fields[13]. The reversible swelling of multi-responsive hydrogels could play a crucial role in nerve excitation, muscle contraction, and cell locomotion.[14-17]

Amphiphilic co-networks (APCNs) composed of hydrophilic and hydrophobic segments phase separate at the nano-scale when swollen in different polar solvents.[18, 19] Thus, APCNs could exhibit unique chemical and physical properties.[20-22] Our research group has prepared well-defined APCN,[23, 24] particularly, poly(ε-caprolactone)-poly(ethylene glycol) (PCL-PEG) hydrogels produced by click chemistry, which have excellent biocompatibility and have been used for carriers for controlled drug release. Another stimuli-responsive hydrogel which responds to pH and ions, are composed of carboxyl group polymer chains such as poly(acrylic acid) (PAA)[25, 26], poly(methacrylic acid) (PMAA)[27] and alginate[28, 29]. These hydrogels absorb divalent ions and possess high performance mechanical properties due to ionic crosslinking between carboxyl groups.[30]

Although stimuli-responsive hydrogels have shown application in tissue engineering as biomaterials, mechanical strength cannot be neglected. The degree of crosslinking, the main influence on the mechanical property of multi-responsive hydrogels, is not only controlled by the double bond conversion in the copolymerization, but also controlled by metal-ligand bonding between divalent cations and side groups of polymer chains.[31] Traditional multi-responsive hydrogels, prepared by random free radical copolymerization of multifunctional crosslinking, have less structural integrity.[23, 32, 33] There are many defects in the network structure which leads to soft, weak and brittle hydrogels, limiting further applications in various fields.[34] Well-defined multi-responsive hydrogels not only exhibit defined polymer molecular weight and high degree of constant crosslinking; they also provide flexible control over structural defects in the network structure. Therefore, well-defined multi-responsive hydrogels are characterized by a high elastic modulus.[35, 36] For example, articular cartilage is unable to be repaired if damaged progressively, and has therefore been substituted with well-defined polyelectrolyte hydrogels, which exhibit biocompatibility, ionic conductivity and high mechanical performance.[37]

Click chemistry and living radical polymerization (LRP) provides efficient methods for preparing well-defined multi-responsive hydrogels. Click chemistry, particularly copper (I)-catalyzed azide-alkyne cycloaddition (CuAAC), has attracted a considerable amount of attention for the preparation of well-defined and high strength hydrogels due to reaction specificity, quantitative yields and functional group tolerance.[38-42] Atom transfer radical polymerization (ATRP) also provides a unique tool for preparing monodispersed and functional polymers with controlled molecular weight. [43-46]

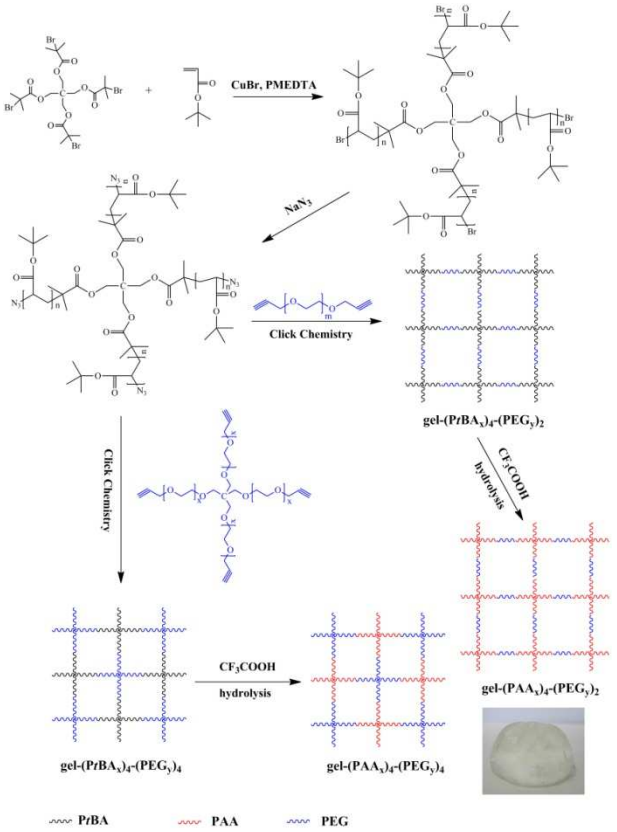

Scheme 1 The gel-$(PAA_x)_4$-$(PEG_y)_4$ and gel-$(PAA_x)_4$-$(PEG_y)_2$ synthetic design strategies.

In this study, well-defined poly(acrylic acid)-poly(ethylene glycol) (PAA-PEG) multi-responsive hydrogels were prepared *via* ATRP and CuAAC. PEG is also a widely utilized biomedical material exhibiting anti-thrombotic function and immunogenic proteins due to its hydrophilicity, biocompatibility.[47, 48] Similarly, poly(acrylic acid) (PAA) is a widely used biomedical polymer, and its conformation in aqueous solution is dependent on the pH value of the solution. Divalent cations cooperatively bind the carboxyl side groups of PAA and create ionic crosslinks.[49, 50] Furthermore, the selection of Ca^{2+} instead of other divalent cationic metal ions in this study is due to the typical level of Ca^{2+} concentration in the human body (1.8 mM), especially, the Ca^{2+} concentration in a human knee joint equivalent to 4.0 mM $CaCl_2$.[51-53] Thus, the multi-responsive PAA-PEG hydrogel (gel-PAA-PEG) is achieved *via* controlling the degree of divalent cationic crosslinking, leading to hydrogels which can be swollen or shrunk reversibly, with a high degree of control.

Experimental

Materials

N,N,N',N',N''-pentamethyldiethylenetriamine (PMDETA, J&K Scientific, 99.9%), sodium azide (NaN_3, Alfa Aesar, 98 %), 2-bromoisobutyryl bromide (Aldrich, 99.9%), 1, 4-dioxane (Shanghai Chemical Reagent, China, 99.9%), pentaerythritol (Shanghai Chemical Reagent, China, 99.9%), trifluoroacetic acid (Shanghai Chemical Reagent, China, 99.9%), calcium chloride ($CaCl_2$, Shanghai Chemical Reagent, China, 99.9%), *N,N*-dimethylformamide (DMF, Shanghai Chemical Reagent, China, 99.9 %), polyethylene glycol (PEG, Aldrich, M_n = 4000), tetra-alkyne terminated polyethylene glycol ($PEG_{56}(C{\equiv}CH))_4$ (Sinopeg Biotech, China, M_n = 10000), RPMI-1640 medium (Gibco, U.S.A), phosphate buffered saline (PBS) (Gibco, U.S.A), 3-(4,5-dimethylthiazol-2-yl)-2,5-diphenyltetrazolium bromide (MTT, Gibco, U.S.A), dimethyl sulfoxide (DMSO, Gibco, U.S.A, Anhydrous) were all used as received; methylene chloride (Shanghai Chemical Reagent, China, 99.9%) was dried with CaH_2 and evaporative refluxed before use; tetrahydrofuran (THF, Shanghai Chemical Reagent, China, 99.9%) was dried with sodium and evaporative refluxed before use, with benzophenone as indicator; propargyl bromide (J&K, 80%) was distilled before use; *t*-butyl acrylate (*t*-BA, Alfa Aesar, 99%) was vacuum distilled before use; cuprous bromide (CuBr, Acros, 98%) was washed with glacial acetic acid to remove soluble oxidized species, filtered, washed with ethanol and finally dried in vacuum.

Synthesis of four-armed (P*t*BA-Br)$_4$ by ATRP

Four-armed core initiator (93.06 mg, 0.137 mmol), *t*-BA (4.0 mL, 27.4 mmol), toluene 1 mL, CuBr (78.8 mg, 0.548 mmol), and PMDETA (96.8 mg, 0.56 mmol) were placed in a 10 mL dry glass ampoule with a magnetic stirring bar. The reaction mixture underwent three successive freeze-pump-thaw cycles to eliminate oxygen, and then the ampoule was sealed under nitrogen atmosphere and placed in a pre-heated oil bath at 60 °C. At a predetermined time, the ampoule was opened to stop the reaction, and the crude product was diluted with about 40 mL methylene chloride, and passed through an Al_2O_3 column to remove the copper and copper salt. The polymer solution was concentrated by rotary evaporation, and precipitated into an excess amount of methanol and water solution (v/v=1/1). This purification process was repeated three times. The sample was obtained by filtration and dried under vacuum at 25 °C overnight. The conversion of the monomer was determined by gravimetry.

Synthesis of azide-terminated four-armed (P*t*BA-N_3)$_4$

Four-armed (P*t*BA-Br)$_4$ (0.22 mmol) was dissolved in *N,N*-dimethylformamide (DMF, 30 mL), stirred for 30 min. Then, sodium azide (8.8 mmol) was added, the reaction mixture was stirred for another 24 h at 30 °C. After reaction, the mixture solution was evaporated to remove DMF. The crude polymer was diluted with 100 mL methylene chloride and passed through an Al_2O_3 column to remove the excessive NaN_3. Finally, the polymer solution was concentrated by rotary evaporation, and precipitated into an excess amount of mixture solution of methanol and water solution (v/v=1/1). The polymer sample was obtained by filtration and dried under vacuum at 25 °C overnight to obtain a white solid.

Preparation of P*t*BA-PEG hydrogel (gel-P*t*BA-PEG) *via* Click Chemistry

The formation of gel-(P*t*BA)$_4$-(PEG)$_2$ samples were as follows: four-armed (P*t*BA-N_3)$_4$ (0.0033 mmol), $(PEG_{45}(C{\equiv}CH))_2$ (M_n=4000) (0.007 mmol), CuBr (0.01 mmol) and 1, 4-dioxane 1 mL were introduced into a small reaction tube. After the polymers dissolved completely, the reaction tube was sealed with nitrogen for 10 min, and PMDETA (0.01 mmol) was quickly injected under ultrasonic agitation. The reaction was allowed to

continue for 24 h at 25 °C. A uniform hydrogel was obtained from the reaction tube. The gel was immersed EDTA solution (5%) to remove the copper ions and DMF. Finally, the gels were fully swollen in large volume of deionized water for two weeks, with the deionized water changed everyday, and dried at 60 °C until constant weight. The preparation of gel-(P*t*BA)$_4$-(PEG)$_4$ sample was similar to that of gel-(P*t*BA)$_4$-(PEG)$_2$.

Synthesis of gel-PAA-PEG and Ca^{2+} composite hydrogels

The gel-P*t*BA-PEG samples were fully swollen in 40 mL dry methylene chloride, and 4 mL trifluoroacetic acid was slowly added. The mixture was stirred at room temperature for 24 h. After removal of trifluoroacetic acid, the gels were fully swollen in large volume of deionized water for two weeks, with the deionized water changed everyday, and dried at 60 °C until constant weight to form gel-PAA-PEG. Then the gel-PAA-PEG samples were completely neutralized by 0.3% NaOH solution, and immersed into various concentrations of Ca^{2+} ($CaCl_2$) solution; the hydrogels were swelled to equilibrium and then the hydrogel surface was washed by deionized water immediately; finally the hydrogels were dried with a freeze-dryer.

Characterization

^{1}H NMR spectra were obtained by AVANCE 400 MHz spectrometer (Bruker, Germany), using the solvent signal for calibration. The P*t*BA, P*t*BA-N_3 products were analyzed using Fourier-transform infrared (FT-IR) spectrometer (Avatar 370, Thermo Fisher Nicolet, U.S.A). The samples were dried completely and ground to a fine power, and blended with KBr. The hydrogels were analyzed by FT-IR spectrometer equipped with ATR accessory at an incident angle of 90°. Molecular weights and molecular weight distributions were determined by gel permeation chromatography (GPC) performed at 40 °C in anhydrous tetrahydrofuran (THF, flow rate 1 mL·min^{-1}), the detection was performed with a Model 2414 differential refractometer detector. The thermal stability of the prepared hydrogels were carried out by thermo gravimetric analyzer (SDT-Q600, TA Instructments) with a temperature range of 50 to 800 °C at heating rate of 10 °C /min under nitrogen atmosphere. The rheological behavior of PAA-PEG hydrogels were performed on MCR 102 Modular Compact Rheometer (Anton Paar, Austria) equipped with parallel plate geometry with a diameter of 25 mm at 25 °C. The gap distance between the two plates was fixed at 1 mm. A frequency sweep test was conducted on each hydrogel to determine values of storage modulus (G') and loss modulus (G'') over a frequency range of 0.1-200 Hz.

Gel-P*t*BA-PEG/gel-PAA-PEG swelling of hydrogels

Swelling behavior of the hydrogels was measured by a gravimetric method. 1.5 g dry gel-P*t*BA-PEG samples were immersed into 1, 4-dioxane and deionized water at 25 °C, respectively. The hydrogels were taken out at certain time intervals, wiped by filter paper and weighed. The pH effect of gel-PAA-PEG samples on swelling ratio were similar to above procession in buffer solutions of desired pH (2.0-10.0) at 25 °C. To investigate the effect of ionic concentration on swelling ratio, 1.5 g gel-PAA-PEG samples were completely neutralized by NaOH solution for 24 hours, and then washed with deionized water three times, the samples were equilibrated in 50 mL of deionized water containing up to 50 mmol/L of $CaCl_2$.

The swelling ratio (SR) of the hydrogels was determined gravimetrically using the following equation (1).

$$SR = (m_t - m_0) / m_0 \times 100\% \quad (1)$$

here m_t is the mass of the swollen hydrogel at time t and m_0 is the original mass of the dry gel.

Degree of Ca^{2+} secondary crosslinking of gel-PAA-PEG

The neutralized gel-PAA-PEG samples (100.0 mg) were added to 100 mL Ca^{2+} ($CaCl_2$) solution of desired concentration at room temperature (25 °C). The degree of secondary crosslinking (DC) kinetics was measured at different time intervals (0 - 7 h) at an initial Ca^{2+} solution concentration 1 mmol/L; DC at different initial Ca^{2+} solution concentrations was measured from 0 to 2.7 mmol/L, and each sample swelled for 7 h. The amount of residual Ca^{2+} in the solution was determined by TAS-990AFG Flame Atom Absorption Spectrophotometer (FAAS) (Persee co., China). The amount of adsorption q (mmol/g), degree of Ca^{2+} secondary crosslinking (Ca^{2+} DC) and adsorbent ratio R were calculated from the follow equations[54].

$$q = (C_0 - C_e) \times V / m \quad (2)$$

$$q_{th} = [1 / [M_n(PAA) + n \times M_n(PEG)]] \times 2000 \times DP \quad (3)$$

$$\text{Degree of } Ca^{2+} \text{ secondary crosslinking (\%)} = q / q_{th} \times 100\% \quad (4)$$

$$R = (C_0V_0 - C_eV_e) / C_0V_0 \times 100\% \quad (5)$$

here C_0 and C_e are the initial and equilibrium Ca^{2+} concentration (mmol/L); m is the mass of adsorbent used (g); M_n(PAA) = M_n(P*t*BA)-4×DP×56; n is feed ratio of PEG and P*t*BA/PAA (the conversion of CuAAC almost 100%); DP is degree of polymerization for per-arm P*t*BA/PAA, V, $V_0 \approx V_e$ (L) are the solution volume.

Measurement of proton conductivity

The conductivity of gel-PAA-PEG with different Ca^{2+} DC at the initial Ca^{2+} solution concentrations of 0 to 2.7 mmol/L were characterized by four-point probe technique with a linear probe head (ST2253 Jingge electronic Co., LTD, China). The bulk resistance of hydrogels (R) was calculated from the applied current (I) and recorded voltage (V), using Ohm's law: R = V / I, with four separate measurements made for each hydrogel. The hydrogels were cut into thin slices with the average thickness of around 1 mm, and the system temperature was controlled at room temperature by a thermocouple heating apparatus. To avoid any possible interference from any solution on the gel surface, the surface solution on the hydrogels was carefully tapped dry, before each measurement.

***In vitro* degradation studies**

Degradation tests were carried out by immersing the gel-PAA-PEG samples in phosphate-buffered saline solution (KH_2PO_4 1.98 mM, Na_2HPO_4 10.00 mM, NaCl 136.89 mM, KCl 2.68 mM, pH=7.4) at 37 °C and the buffer solution was changed every day. After a predetermined time, the samples were removed from the solution, washed thoroughly with distilled water, dried completely in a vacuum oven at 60 °C and the final mass obtained. The percentage of the mass loss was calculated from

eqn (6).[55]

$$\text{Mass loss (\%)} = (m_i - m_d) / m_i \times 100\% \quad (6)$$

here m_i is the initial dry hydrogel mass and m_d is the hydrogel mass after degradation at a certain time. The mass loss was measured in the buffer solution for each hydrogel sample as a function of time.

MTT viability assay

MTT viability assay was used to assess the relative cytotoxicity of the prepared gel-PAA-PEG hydrogels. All hydrogels were sterilized prior to cell culture by immersion in 70% ethanol for 2 h, and then rinsed 5 times with sterile phosphate buffer saline (PBS) (pH = 7.4) to remove residual alcohol, and further sterilized by UV for 1 h. The gel-PAA-PEG hydrogels were extracted with RPMI-1640 (0.1 g / mL) for 24 h, respectively. The extracts were collected as conditioned medium for the cell viability tests. The as prepared L929 cells were seeded onto 96-well plates at 1×10^4 viable cells per well and incubated with conditioned media in a humidified 5% CO_2 atmosphere at 37 °C for 24 h and 48 h, respectively. Negative and positive control groups were filled with treated samples, RPMI-1640 medium, and phenol solution, respectively. After incubation for 24 h and 48 h, 15 μL of MTT stock solution in PBS (5 mg·mL^{-1}) was added to each well at 37 °C. After 4 h, the MTT solution was removed and 150 μL DMSO was added to each well to dissolve formazan crystals. The optical density (OD) of the wells was determined at 570 nm using a multifunctional microplate reader. Experiments were performed in triplicate and were repeated at least twice. The relative cell viability (%) was calculated as eqn (7).

$$\text{Cell viability} = (OD_{test} - OD_{blank}) / (OD_{control} - OD_{blank}) \times 100\% \quad (7)$$

where OD_{test} is the experiment group optical density; $OD_{control}$ is the negative group optical density (OD); OD_{blank} is the blank group optical density (OD). The cell MTT viability in the three experimental groups was compared with the negative and positive groups.

Results and Discussion

Synthesis of PAA-PEG hydrogel

Synthesis of four-armed P*t*BA by ATRP and end group azide modification

Based upon earlier work,[56, 57] four-armed poly(*tert*-butyl acrylate) (P*t*BA), a protected precursor of four-armed poly(acrylic acid) (PAA), was synthesized by ATRP. Initially *tert*-butyl acrylate and four-armed core initiator were employed (Scheme 1). Typically, the polymerizations of (P*t*BA-Br)$_4$ were carried out at 60 °C, in the presence of a catalyst system of CuBr/PMDETA using toluene as solvent. After polymerization, the as prepared bromide end groups of the (P*t*BA-Br)$_4$ were converted into the azido group in the presence of excess NaN_3 in DMF at 30 °C. Fig. S1 (supporting information) shows the GPC trace of well defined four-armed P*t*BA at different polymerization times, which exhibits two single peaks, and indicates the higher molecular weight with longer polymerization times. The characteristics of the polymers obtained are given in Table S1. As shown in Table S1, the polymerization could be controlled with 73% of monomer conversion in 4 h and 92% of monomer conversion in 15 h,

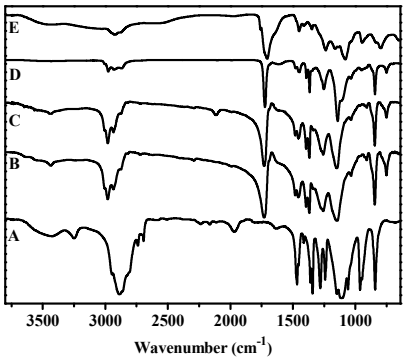

Fig. 1 FT-IR spectra of (A) $(PEG_{45}(C\equiv CH))_2$, (B) $(PtBA_{41}\text{-}Br)_4$, (C) $(PtBA\text{-}N_3)_4$, (D) gel-$(PtBA_{41})_4$-$(PEG_{45})_2$, (E) gel-$(PAA_{41})_4$-$(PEG_{45})_2$.

respectively. The ^{1}H NMR spectrum of four-armed P*t*BA polymer is shown in Fig. S2, and the expected peaks attributed to four-armed P*t*BA can be clearly detected. The degree of polymerization for the four-armed P*t*BA polymer named $(PtBA_{41})_4$ ($M_{n(NMR)}$ = 21100, DP = 164) and $(PtBA_{78})_4$ ($M_{n(NMR)}$ = 40100, DP=312) which was calculated by ^{1}H NMR from the integration of the signals at 1.44 ppm (H^c) which corresponds to the protons of the *t*-butyl group and the signals at 1.25 ppm (H^d) corresponds to the protons of initiator. The results are close to the theoretical value $M_{n(th)}$, and also demonstrate the ATRP of *t*-BA initiated with four-armed core initiator was well controlled. The azide-terminated polymers $(PtBA_{41}\text{-}N_3)_4$ were confirmed with the FT-IR spectra (Fig. 1 C). Compared with the FT-IR spectrum of $(PtBA_{41}\text{-}Br)_4$, a new absorption peak at 2100 cm^{-1} appeared which indicated the bromide groups at the end of four-armed P*t*BA chain had been converted to azide end groups successfully.

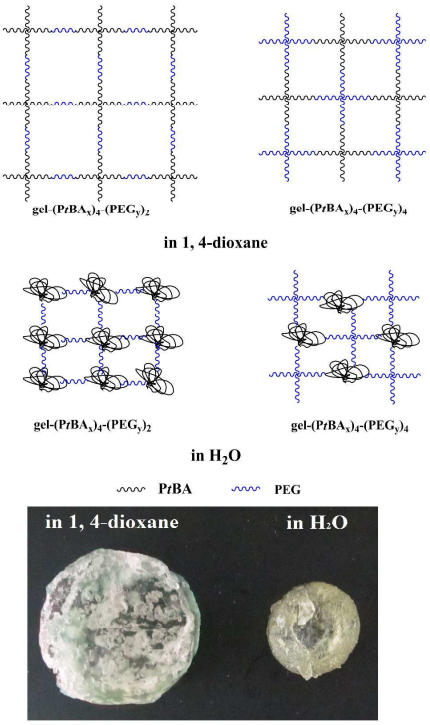

Scheme 2 Gel-(P*t*BA$_x$)$_4$-(PEG$_y$)$_2$ and gel-(P*t*BA$_x$)$_4$-(PEG$_y$)$_4$ in different solutions.

Synthesis of PAA-PEG hydrogel by click chemistry

"Click" chemistry was used to prepare the P*t*BA-PEG network between four-armed (P*t*BA-N$_3$)$_4$ and (PEG$_{45}$(C≡CH))$_2$ / (PEG$_{56}$(C≡CH))$_4$. It is worth noting that the stretch peak of C≡*C*-*H* group at 3300 cm^{-1} of (PEG$_{45}$(C≡CH))$_2$ and azide groups of (P*t*BA$_{41}$-N$_3$)$_4$ at 2100 cm^{-1} completely disappeared from the IR spectrum of gel-(P*t*BA$_{41}$)$_4$-(PEG$_{45}$)$_2$ in Fig. 1 D, which confirms the completed reaction between azide groups and alkyne groups. The *t*-butyl acrylate groups of the gel-(P*t*BA$_{41}$)$_4$-(PEG$_{45}$)$_2$ were converted into carboxyl groups by selective hydrolysis with trifluoroacetic acid in dichloromethane to prepare gel-(PAA$_{41}$)$_4$-(PEG$_{45}$)$_2$. Fig. 1 E shows the FT-IR spectra of gel-(PAA$_{41}$)$_4$-(PEG$_{45}$)$_2$ after hydrolysis where a broad band can be observed from 2400 cm^{-1} to 3700 cm^{-1} account for the O-H stretch of carboxylic acid, which confirmed the conversion of the *tert*-butyl ester to the carboxylic acid.[58]

Swelling Behavior

P*t*BA-PEG hydrogels are amphiphilic co-networks (APCNs) composed of hydrophilic (PEG) and hydrophobic (P*t*BA) polymer chains, which are interconnected with chemical crosslinkings as shown in scheme 2. 1, 4-dioxane is a good solvent for both PEG and P*t*BA polymer chains, which P*t*BA-PEG co-networks can be fully swelled in 12 h. Fig. 2 (a) shows gel-(P*t*BA$_{78}$)$_4$-(PEG$_{45}$)$_2$ has a maximum swelling ratio (SR) of 1310%, which is larger than gel-(P*t*BA$_{41}$)$_4$-(PEG$_{45}$)$_2$ (SR = 660%) and gel-(P*t*BA$_{41}$)$_4$-(PEG$_{56}$)$_4$ (SR = 460%). This is attributed to the lower density of crosslinking in gel-(P*t*BA$_{78}$)$_4$-(PEG$_{45}$)$_2$ compared to gel-(P*t*BA$_{41}$)$_4$-(PEG$_{45}$)$_2$ and gel-(P*t*BA$_{41}$)$_4$-(PEG$_{56}$)$_4$. Fig. 2 (b) shows the SR of the P*t*BA-PEG hydrogels in water, which is a good solvent for the PEG segments but poor solvent for P*t*BA. The SR value of gel-(P*t*BA$_{41}$)$_4$-(PEG$_{45}$)$_2$, gel-(P*t*BA$_{78}$)$_4$-(PEG$_{45}$)$_2$ and gel-(P*t*BA$_{41}$)$_4$-(PEG$_{56}$)$_4$ hydrogels in water are 90%, 65%, 127%, respectively, which was dependent on the content of PEG in APCNs.

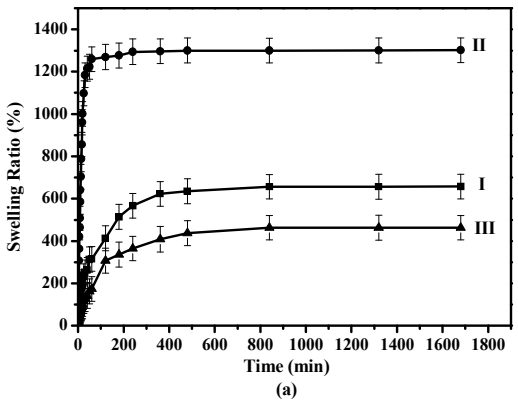

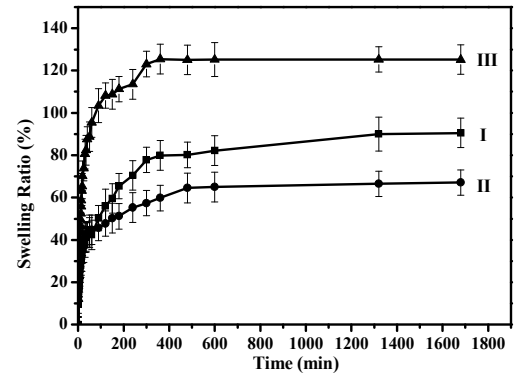

Fig. 2 Swelling Ratio of (I) gel-(P*t*BA$_{41}$)$_4$-(PEG$_{45}$)$_2$, (II) gel-(P*t*BA$_{78}$)$_4$-(PEG$_{45}$)$_2$ and (III) gel-(P*t*BA$_{41}$)$_4$-(PEG$_{56}$)$_4$ in (a) 1, 4-dioxane and (b) H$_2$O.

Hydrolysis of the P*t*BA-PEG yielded the PAA-PEG hydrogel. Fig. 3 (a) shows the SR of PAA-PEG hydrogels in water. As water is a good solvent for both the PAA and PEG polymer chains, the PAA-PEG hydrogels were fully swollen. At neutral pH the SR of gel-(PAA$_{78}$)$_4$-(PEG$_{45}$)$_2$ was much larger than gel-(PAA$_{41}$)$_4$-(PEG$_{45}$)$_2$ and gel-(PAA$_{41}$)$_4$-(PEG$_{56}$)$_4$. This can be attributed to the lower crosslinking density of gel-(PAA$_{78}$)$_4$-(PEG$_{45}$)$_2$ and more defects in the gel-(PAA$_{78}$)$_4$-(PEG$_{45}$)$_2$ structure due to its steric effects between (P*t*BA$_{78}$-N$_3$)$_4$ and (PEG$_{45}$(C≡CH))$_2$.

PAA hydrogel is pH sensitive and can undergo a volume change with changes in pH, as shown in Scheme 3. Fig. 3 (b) shows the pH dependence of the SR of PAA-PEG hydrogels. The SR at pH<4 for the PAA-PEG hydrogels was lower than that at pH>4. Such differences in hydrogel swelling response can be attributed to the ionic strength and electrochemical interactions in the solution. At low pH, -COO$^-$ groups of the PAA chains in the hydrogel can convert into hydrophobic -COOH groups, shrinking

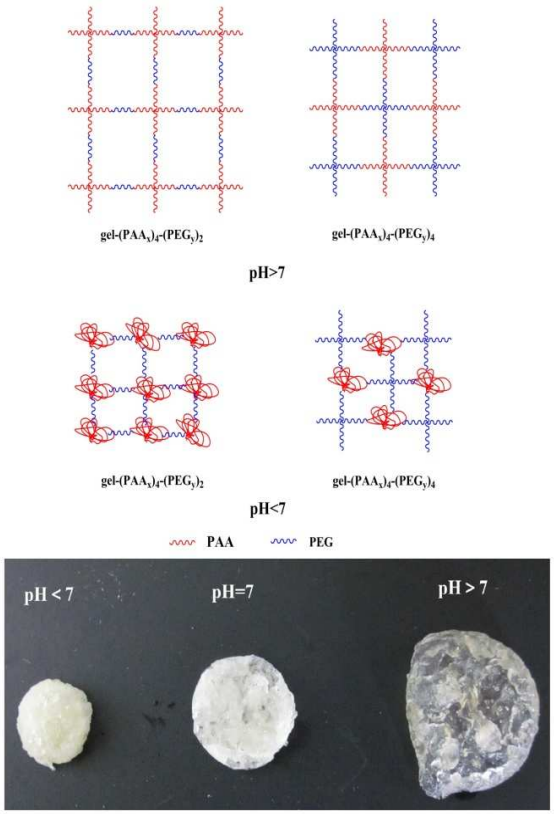

Scheme 3 Gel-$(PAA_x)_4$-$(PEG_y)_2$ and gel-$(PAA_x)_4$-$(PEG_y)_4$ in different pH solutions.

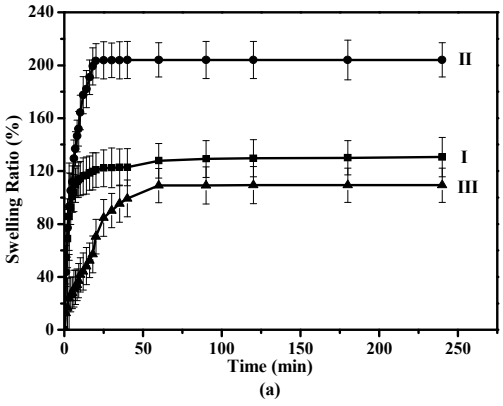

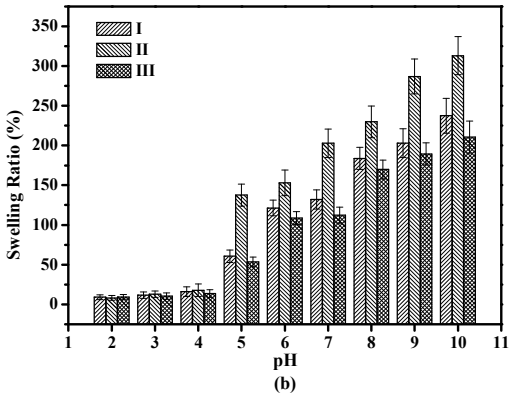

Fig. 3 Swelling ratio for (a) (I) gel-$(PAA_{41})_4$-$(PEG_{45})_2$, (II) gel-$(PAA_{78})_4$-$(PEG_{45})_2$ and (III) gel-$(PAA_{41})_4$- $(PEG_{56})_4$ in water and (b) as a function of pH.

the PAA chains, and undergoing strong hydrogen bonding with the PEG chains. As pH increased from pH=5 to 10, more -COOH groups in the hydrogels formed a polyelectrolyte complex and the hydrogen bonding between -COOH groups and PEG chains was disrupted, causing polymer chain repulsion in the hydrogel and a rapid increase in the swelling ratio. The SR of gel-$(PAA_{78})_4$-$(PEG_{45})_2$ is larger than gel-$(PAA_{41})_4$-$(PEG_{45})_2$, and gel-$(PAA_{41})_4$-$(PEG_{56})_4$ under basic conditions because more -COOH groups in

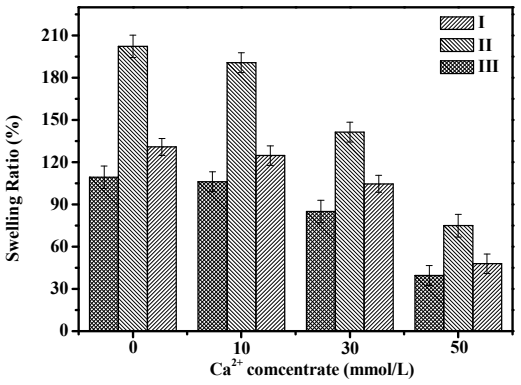

Fig. 4 Swelling ratio of (I) gel-$(PAA_{41})_4$-$(PEG_{45})_2$, (II) gel-$(PAA_{78})_4$-$(PEG_{45})_2$ and (III) gel-$(PAA_{41})_4$-$(PEG_{56})_4$ in different content of Ca^{2+} solution.

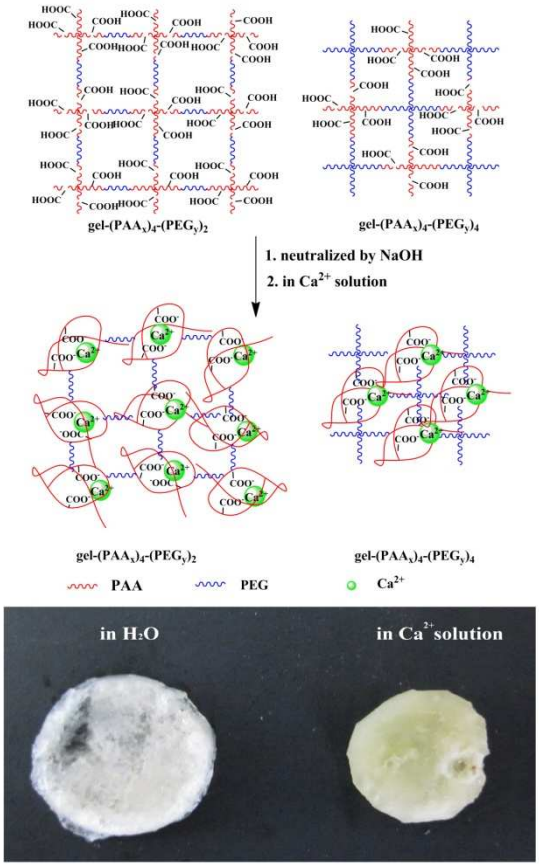

Scheme 4 The gel-(P*t*BA$_x$)$_4$-(PEG$_y$)$_2$ and gel-(P*t*BA$_x$)$_4$-(PEG$_y$)$_4$ in Ca^{2+} solution.

PAA transformed into -COO$^-$, with PAA polymer chains increase, and also due to its larger mesh size.

Fig. 4 shows the effect of different Ca^{2+} concentrations on the swelling of the neutralized PAA-PEG hydrogels. When the Ca^{2+} concentration was less than 10 mmol/L, the swelling ratio of PAA-PEG hydrogels decreased slowly at a level of less than 12%. At Ca^{2+} concentrations above 10 mmol/L, the SR of hydrogels decreased dramatically due to the presence of higher concentration of Ca^{2+} in the solution surrounding the hydrogel, counteracted by the mutual repulsion of the Ca^{2+} on the internal hydrogel as shown in Scheme 4.[59] Conversely, the PAA-PEG hydrogels consisting of ionized polymer chains was deswollen when the charge density increased, thus generating electrostatic interactions between Ca^{2+} and PAA chains.[60, 61] The SR of gel-(PAA$_{78}$)$_4$-(PEG$_{45}$)$_2$ decreased more dramatically than that of gel-(PAA$_{41}$)$_4$-(PEG$_{45}$)$_2$ and gel-(PAA$_{41}$)$_4$-(PEG$_{56}$)$_4$. This is consistent with the increase number of PAA in the hydrogel and the complex formation of PAA chain - Ca^{2+} interactions including intra- and inter-molecular complex formation, which increases the crosslinking density of the hydrogel and restrains the swelling of the hydrogel.[62]

Ca^{2+} secondary crosslinking capacity

Efficient secondary crosslinking time is a very important parameter in adsorption processes and rapid adsorption of Ca^{2+} by a hydrogel is necessary in many applications. Fig. 5 illustrates the degree of Ca^{2+} secondary crosslinking (Ca^{2+} DC) for neutralized PAA-PEG hydrogels as a function of contact time. The Ca^{2+} DC for gel-(PAA$_{78}$)$_4$-(PEG$_{45}$)$_2$ was 12% at the adsorption equilibrium, which was lower than that of gel-(PAA$_{41}$)$_4$-(PEG$_{45}$)$_2$ 14% and gel-(PAA$_{41}$)$_4$-(PEG$_{56}$)$_4$ 13% within 7 h. The as prepared gel-(PAA$_{78}$)$_4$-(PEG$_{45}$)$_2$ has a large amount of acrylic acid groups, which is responsible for its low degree of Ca^{2+} secondary crosslinking. Fig. 6 shows the Ca^{2+} DC for neutralized PAA-PEG hydrogels at different initial Ca^{2+} solution concentrations. The Ca^{2+} DC for gel-(PAA$_{78}$)$_4$-(PEG$_{45}$)$_2$ was from 4% to 12%, at the initial Ca^{2+} content from 0.45 to 0.9 mmol/L in solution, which is lower than that for gel-(PAA$_{41}$)$_4$-(PEG$_{45}$)$_2$ hydrogel and gel-(PAA$_{41}$)$_4$-(PEG$_{56}$)$_4$. However, the Ca^{2+} DC for gel-(PAA$_{78}$)$_4$-(PEG$_{45}$)$_2$ was higher than other two hydrogels, up to 55%, when the initial Ca^{2+} content is 2.7 mmol/L, which can be attributed to its low chemical crosslinking density and easy Ca^{2+} permeation. This rapid crosslinking capacity is consistent with the Ca^{2+} adsorption ratio of the hydrogels in Fig. S3.

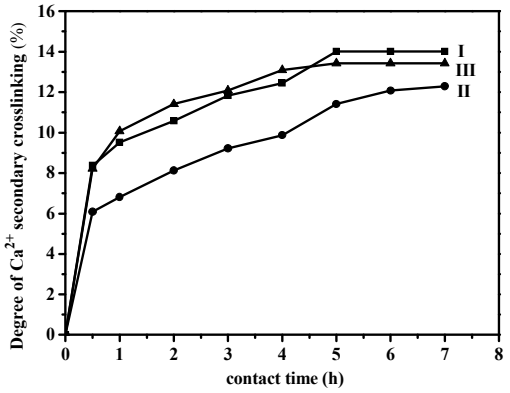

Fig. 5 Degree of Ca^{2+} secondary crosslinking kinetics for (I) gel-(PAA$_{41}$)$_4$-(PEG$_{45}$)$_2$, (II) gel-(PAA$_{78}$)$_4$-(PEG$_{45}$)$_2$ and (III) gel-(PAA$_{41}$)$_4$-(PEG$_{56}$)$_4$. (C$_o$= 1 mmol/L; t= 0-7 h)

Proton conductivity of the hydrogels

In order to investigate the influence of Ca^{2+} DC on the electrical conductivity for the polyelectrolyte hydrogels, the three types of PAA-PEG hydrogels were immersed at the initial Ca^{2+} solution concentrate from 0 to 2.7 mmol/L. Fig. 7 shows the conducti-

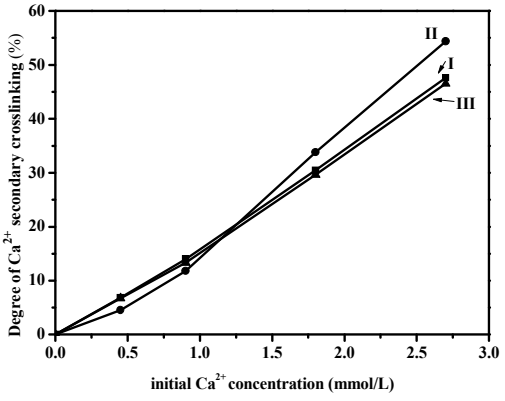

Fig. 6 Degree of Ca^{2+} secondary crosslinking as a function of initial Ca^{2+} concentration for (I) gel-(PAA$_{41}$)$_4$-(PEG$_{45}$)$_2$, (II) gel-(PAA$_{78}$)$_4$-(PEG$_{45}$)$_2$ and (III) gel-(PAA$_{41}$)$_4$-(PEG$_{56}$)$_4$. (C$_o$= 0-2.7mmol/L, t=7 h)

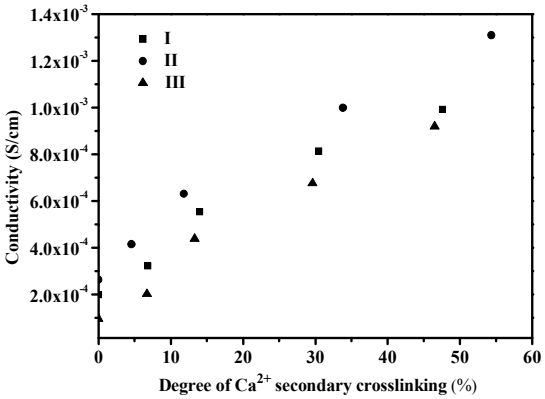

Fig. 7 Conductivity of hydrogels (I) gel-$(PAA_{41})_4$-$(PEG_{45})_2$, (II) gel-$(PAA_{78})_4$-$(PEG_{45})_2$ and (III) gel-$(PAA_{41})_4$-$(TAPEG_{56})_4$ contained different Ca^{2+} DC. (C_o= 0-2.7mmol/L; t=7 h)

vity of the hydrogels with different Ca^{2+} DC. The measured conductivity of the gel-$(PAA_{41})_4$-$(PEG_{45})_2$, gel-$(PAA_{78})_4$-$(PEG_{45})_2$ and gel-$(PAA_{41})_4$-$(PEG_{56})_4$ swelled in deionized water at room temperature were 1.99×10^{-4}, 3.63×10^{-4} and 9.68×10^{-5} S/cm, respectively, indicating the main contribution of increased conduction from the related PAA content increasing in the hydrogel. The conductivity of the PAA-PEG hydrogels dramatically increased with an increase of Ca^{2+} DC, especially the conductivity of gel-$(PAA_{78})_4$-$(PEG_{45})_2$, which contained more than 30% Ca^{2+} DC. This was attributed to calcium ions complexing with the carboxylate ions to form electron transfer channels.

Rheological behavior

Fig. 8 (a) shows the dynamic rheological behavior of PAA-PEG hydrogels swelled in water with the frequency range from 0.1 to 200 Hz. The storage modulus (G') was greater than the loss modulus (G'') over the entire range of testing frequencies. The G' and G'' curves of gel-$(PAA_{41})_4$-$(PEG_{56})_4$ were much higher than those of gel-$(PAA_{41})_4$-$(PEG_{45})_2$ and gel-$(PAA_{78})_4$-$(PEG_{45})_2$ suggesting that gel-$(PAA_{41})_4$-$(PEG_{56})_4$ has a higher crosslinking density between $(PAA_{41})_4$ and $(PEG_{56}(C\equiv CH))_4$ after CuAAC. The dynamical rheological behavior of PAA-PEG hydrogels with different degrees of Ca^{2+} secondary crosslinking in the frequency range from 0.1 to 200 Hz is shown in Fig. 8 (b). The most profound change occurred with the dynamic rheological behavior of PAA-PEG hydrogels with different Ca^{2+} DC. The G' and G'' plateaus greatly shifted upward due to Ca^{2+} acting as ionic secondary crosslinking forming bridges between neighboring PAA chains and modifying the effective interactions between the polymer and ion solution.[63] Although the Ca^{2+} DC of gel-$(PAA_{41})_4$-$(PEG_{56})_4$ is 46%, the chemical crosslinking is much stronger than ion secondary crossliking.

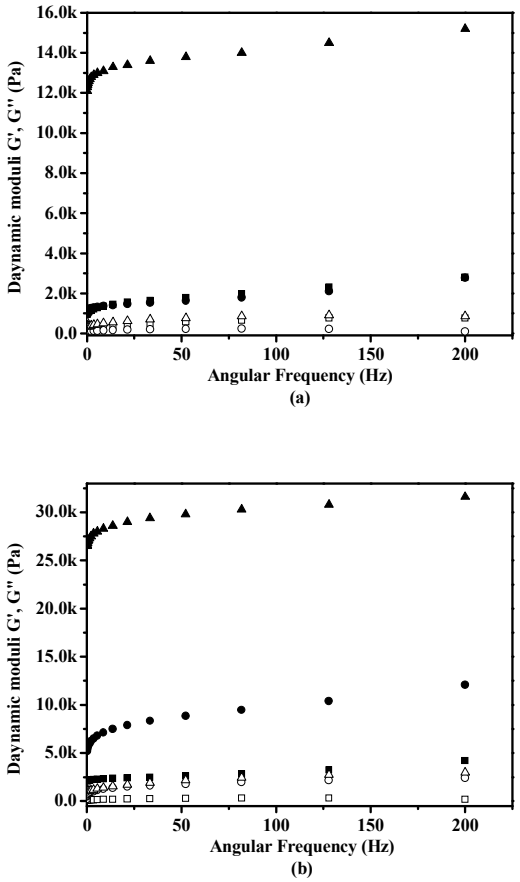

Fig. 8 Storage modulus G' (solid) and loss modulus G'' (open) for hydrogels (a) gel-$(PAA_{41})_4$-$(PEG_{45})_2$ (square), gel-$(PAA_{78})_4$-$(PEG_{45})_2$ (circular) and gel-$(PAA_{41})_4$-$(PEG_{56})_4$ (triangle) as a function of frequency in water; (b) gel-$(PAA_{41})_4$-$(PEG_{45})_2$ 48% Ca^{2+} DC (square), gel-$(PAA_{78})_4$-$(PEG_{45})_2$ contained 55% Ca^{2+} DC (circular) and gel-$(PAA_{41})_4$-$(PEG_{56})_4$ contained 46% Ca^{2+} DC (triangle).

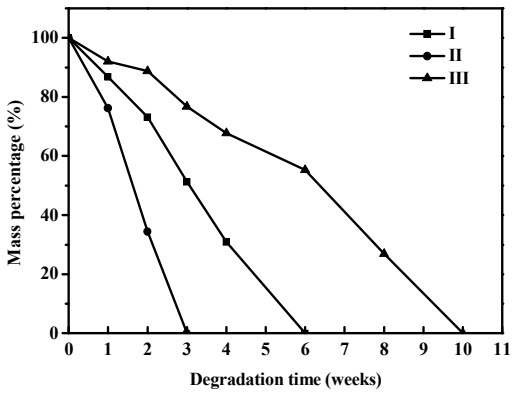

Fig. 9 Mass loss profiles of hydrogels (I) gel-$(PAA_{41})_4$-$(PEG_{45})_2$, (II) gel-$(PAA_{78})_4$-$(PEG_{45})_2$ and (III) gel-$(PAA_{41})_4$-$(PEG_{56})_4$ as a function of degradation time.

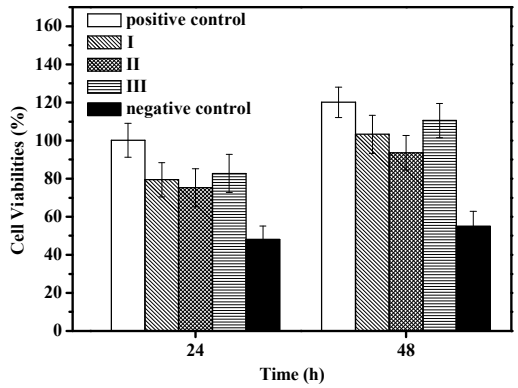

Fig. 10 MTT assay for cytotoxicity of hydrogels (I) gel-$(PAA_{41})_4$-$(PEG_{45})_2$, (II) gel-$(PAA_{78})_4$-$(PEG_{45})_2$, (III) gel-$(PAA_{41})_4$-$(PEG_{56})_4$ in L929 cell culture.

Degradation and cytotoxicity of PAA-PEG hydrogels

The degradation of PAA-PEG hydrogels were carried in PBS solution at pH 7.4 and 37 °C (Fig. 9). The mass loss of the gel-$(PAA_{41})_4$-$(PEG_{56})_4$ reaches 100% decomposition (10 weeks), which is slower than that of gel-$(PAA_{78})_4$-$(PEG_{45})_2$ (3 weeks) and gel-$(PAA_{41})_4$-$(PEG_{45})_2$ (6 weeks). The longer degradation time of gel-$(PAA_{41})_4$-$(PEG_{56})_4$ might be ascribed to lower water swelling capability and slower hydrolysis of ester groups (formed from the reaction between pentaerythritol and 2-bromoisobutyryl bromide) at the intersection of four-armed initiator.

To assess the biocompatibility of the hydrogels, the *in vitro* cell viability of the extracted leached media from PAA-PEG hydrogels was evaluated by MTT assay using L-929 cell line. Fig. 10 shows the MTT assay for cytotoxicity of gel-$(PAA_{41})_4$-$(PEG_{45})_2$, gel-$(PAA_{78})_4$-$(PEG_{45})_2$, gel-$(PAA_{41})_4$-$(PEG_{56})_4$ and control experiments in L929 cells after incubation for 24 and 48 h, respectively. All cell viabilities of hydrogels were greater than 70%. It is worth noting that the cell viability of gel-$(PAA_{41})_4$-$(PEG_{56})_4$ reached 83% and 111% after treatment for 24 h and 48 h, respectively, which is higher than that of gel-$(PAA_{41})_4$-$(PEG_{45})_2$ and gel-$(PAA_{78})_4$-$(PEG_{45})_2$. Therefore, the prepared PAA-PEG hydrogel showed good biocompatibility with L929 cells and even accelerated cell growth.

Conclusions

The combination of ATRP and CuAAC demonstrates a flexible method to design different structures of well-defined multi-responsive PAA-PEG hydrogels. The structures of well-defined PAA-PEG hydrogels displayed a pH response in swelling. Furthermore, the PAA-PEG hydrogels not only have excellent biodegradation, but have certain ability to control the crosslinking with Ca^{2+}. The well-defined PAA-PEG hydrogels contained Ca^{2+} enhanced the degree of secondary crosslinking, increased conductivity and improved the rheological behavior. MTT assay also showed cell viabilities of PAA-PEG hydrogels exceeding 70% after treatment for 24 h and 48 h. These unique properties allow the functional hydrogels as potential biomaterials for the fabrication of tissue-engineered cartilage constructs.

Acknowledgements

This work was supported by National Natural Science Foundation of China (No. 21274020 and No. 21304019).

Notes and references

[a] *School of Chemistry and Chemical Engineering, Southeast University, Nanjing, Jiangsu Province, 211189, China. Fax: (+86) 25-52090625; Tel: (+86) 25-52090625; E-mail: fu7352@seu.edu.cn*
[b] *School of Public Health, Southeast University, Nanjing, Jiangsu Province , 210009, China.*
[c] *Department of Materials Engineering, Monash University, Clayton, Victoria, 3800, Australia. Fax: (+61) 3 990 54909; Tel: (+61) 3 990 59609; E-mail: john.forsythe@monash.edu*

† Electronic Supplementary Information (ESI) available: Details of synthesis of four-armed core initiator and di-alkyne terminated PEG $(DAPEG_{45})_2$, structural characterizations of P*t*BA, Ca^{2+} absorption ratio of hydrogels and Thermo gravimetric analysis (TGA). See DOI: 10.1039/b000000x/

1. H. H. Cho, D.-W. Han, K. Matsumura, S. Tsutsumi and S.-H. Hyon, *Biomaterials*, 2008, **29**, 884-893.
2. S. Prabhu and S. Hossainy, *J. Biomed. Mater. Res., Part A*, 2007, **80**, 732-741.
3. V. Kozlovskaya, E. Kharlampieva, I. Erel and S. A. Sukhishvili, *Soft Matter*, 2009, **5**, 4077-4087.
4. K. Y. Lee and D. J. Mooney, *Chem. Rev.*, 2001, **101**, 1869-1880.
5. G. Erdodi and J. P. Kennedy, *J. Polym. Sci., Part A: Polym. Chem.*, 2005, **43**, 4953-4964.
6. J. Grignon and A. Scallan, *J. Appl. Polym. Sci.*, 1980, **25**, 2829-2843.
7. A. S. Hoffman, *J. Controlled Release*, 1987, **6**, 297-305.
8. J. Ricka and T. Tanaka, *Macromolecules*, 1984, **17**, 2916-2921.
9. Y. Li and T. Tanaka, *J. Chem. Phys.*, 1990, **92**, 1365.
10. J. Hrouz, M. Ilavský, K. Ulbrich and J. Kopeček, *Eur. Polym. J.*, 1981, **17**, 361-366.
11. S. Katayama, Y. Hirokawa and T. Tanaka, *Macromolecules*, 1984, **17**, 2641-2643.
12. T. G. Park and A. S. Hoffman, *Macromolecules*, 1993, **26**, 5045-5048.
13. S. R. Eisenberg and A. J. Grodzinsky, *J. Membr. Sci.*, 1984, **19**, 173-194.
14. N. A. Peppas, J. Z. Hilt, A. Khademhosseini and R. Langer, *Adv. Mater.*, 2006, **18**, 1345-1360.
15. F. Brandl, F. Sommer and A. Goepferich, *Biomaterials*, 2007, **28**, 134-146.
16. S. Yang, G. Liu, Y. Cheng and Y. Zheng, *J. Macromol. Sci., Part A: Pure Appl. Chem.*, 2009, **46**, 1078-1082.
17. F. Horkay, I. Tasaki and P. J. Basser, *Biomacromolecules*, 2000, **1**, 84-90.
18. T. K. Georgiou, M. Vamvakaki and C. S. Patrickios, *Polymer*, 2004, **45**, 7341-7355.
19. M. Vamvakaki and C. S. Patrickios, *J. Phys. Chem. B*, 2001, **105**, 4979-4986.
20. G. Erdodi and J. P. Kennedy, *Prog. Polym. Sci.*, 2006, **31**, 1-18.
21. L. Mespouille, J. L. Hedrick and P. Dubois, *Soft Matter*, 2009, **5**, 4878-4892.
22. I. Gitsov, *J. Polym. Sci., Part A: Polym. Chem.*, 2008, **46**, 5295-5314.
23. C. Zhou, S. Qian, A. Zhang, L. Xu, J. Zhu, Z. Cheng, E. T. Kang, F. Yao and G. D. Fu, *RSC Adv.*, 2014, **4**, 8144-8156.

24. Y. Yuan, A. K. Zhang, J. Ling, L.-H. Yin, Y. Chen and G. D. Fu, *Soft Matter*, 2013, **9**, 6309-6318.
25. N. Stavrouli, I. Katsampas, S. Aggelopoulos and C. Tsitsilianis, *Macromol. Rapid Commun.*, 2008, **29**, 130-135.
26. Z. Wei, J. He, T. Liang, H. Oh, J. Athas, Z. Tong, C. Wang and Z. Nie, *Polym. Chem.*, 2013, **4**, 4601-4605.
27. K. J. Henderson, T. C. Zhou, K. J. Otim and K. R. Shull, *Macromolecules*, 2010, **43**, 6193-6201.
28. J. Y. Sun, X. Zhao, W. R. Illeperuma, O. Chaudhuri, K. H. Oh, D. J. Mooney, J. J. Vlassak and Z. Suo, *Nature*, 2012, **489**, 133-136.
29. S. Zhou, A. Bismarck and J. H. Steinke, *J. Mater. Chem. B*, 2013, **1**, 4736-4745.
30. Y. Zhao, J. Kang and T. Tan, *Polymer*, 2006, **47**, 7702-7710.
31. J. E. Elliott, M. Macdonald, J. Nie and C. N. Bowman, *Polymer*, 2004, **45**, 1503-1510.
32. M. Lutolf and J. Hubbell, *Nat. Biotechnol.*, 2005, **23**, 47-55.
33. N. Zagris, *Micron*, 2000, **32**, 427-438.
34. J. P. Gong, *Soft Matter*, 2010, **6**, 2583-2590.
35. G. Hild, *Prog. Polym. Sci.*, 1998, **23**, 1019-1149.
36. N. Sahiner, M. Singh, D. De Kee, V. T. John and G. L. McPherson, *Polymer*, 2006, **47**, 1124-1131.
37. M. Dadsetan, M. Pumberger, M. E. Casper, K. Shogren, M. Giuliani, T. Ruesink, T. E. Hefferan, B. L. Currier and M. J. Yaszemski, *Acta Biomater.*, 2011, **7**, 2080-2090.
38. P. Wu, A. K. Feldman, A. K. Nugent, C. J. Hawker, A. Scheel, B. Voit, J. Pyun, J. M. Frechet, K. B. Sharpless and V. V. Fokin, *Angew. Chem. Int. Ed.*, 2004, **43**, 3928-3932.
39. W. H. Binder and R. Sachsenhofer, *Macromol. Rapid Commun.*, 2007, **28**, 15-54.
40. J. A. Johnson, M. Finn, J. T. Koberstein and N. J. Turro, *Macromol. Rapid Commun.*, 2008, **29**, 1052-1072.
41. V. Crescenzi, L. Cornelio, C. Di Meo, S. Nardecchia and R. Lamanna, *Biomacromolecules*, 2007, **8**, 1844-1850.
42. D. A. Ossipov and J. Hilborn, *Macromolecules*, 2006, **39**, 1709-1718.
43. T. E. Patten and K. Matyjaszewski, *Adv. Mater.*, 1998, **10**, 901-915.
44. V. Coessens, T. Pintauer and K. Matyjaszewski, *Prog. Polym. Sci.*, 2001, **26**, 337-377.
45. J. Pyun, T. Kowalewski and K. Matyjaszewski, *Macromol. Rapid Commun.*, 2003, **24**, 1043-1059.
46. K. Matyjaszewski and J. Xia, *Chem. Rev.*, 2001, **101**, 2921-2990.
47. G. M. Whitesides, E. Ostuni, S. Takayama, X. Jiang and D. E. Ingber, *Annu. Rev. Biomed. Eng.*, 2001, **3**, 335-373.
48. M. Malkoch, R. Vestberg, N. Gupta, L. Mespouille, P. Dubois, A. F. Mason, J. L. Hedrick, Q. Liao, C. W. Frank and K. Kingsbury, *Chem. Commun.*, 2006, 2774-2776.
49. N. Sahiner, *Prog. Polym. Sci.*, 2013, **38**, 1329-1356.
50. X. Liu, S. Luo, J. Ye and C. Wu, *Macromolecules*, 2012, **45**, 4830-4838.
51. A. P. Quist, S. K. Rhee, H. Lin and R. Lal, *J. Cell Biol.*, 2000, **148**, 1063-1074.
52. T. Yamaguchi, N. Chattopadhyay, O. Kifor, J. L. Sanders and E. M. Brown, *Biochem. Biophys. Res. Commun.*, 2000, **279**, 363-368.
53. L. Q. Wan, J. Jiang, D. E. Arnold, X. E. Guo, H. H. Lu and V. C. Mow, *Cell. Mole. Bioeng.*, 2008, **1**, 93-102.
54. Y. Zheng, D. Huang and A. Wang, *Anal. Chim. Acta*, 2011, **687**, 193-200.
55. X. Wen, X. Cao, Z. Yin, T. Wang and C. Zhao, *Carbohydr. Polym.*, 2009, **78**, 193-198.
56. W. Zhang, W. Zhang, J. Zhu, Z. Zhang and X. Zhu, *J. Polym. Sci., Part A: Polym. Chem.*, 2009, **47**, 6908-6918.
57. L. A. Connal, Q. Li, J. F. Quinn, E. Tjipto, F. Caruso and G. G. Qiao, *Macromolecules*, 2008, **41**, 2620-2626.
58. O. Chapman, *J. Am. Chem. Soc.*, 1963, **85**, 3316-3316.
59. Flory and P. J., *Principles of polymer chemistry*, Cornell University Press, 1953.
60. G. Bokias, G. Staikos and I. Iliopoulos, *Polymer*, 2000, **41**, 7399-7405.
61. A. R. Khokhlov and E. Y. Kramarenko, *Macromolecules*, 1996, **29**, 681-685.
62. B. L. Rivas, E. D. Pereira and I. Moreno-Villoslada, *Prog. Polym. Sci.*, 2003, **28**, 173-208.
63. R. Jing and H. Hongfei, *Eur. Polym. J.*, 2001, **37**, 2413-2417.

TOC Graphics

Title: Synthesis and Characterization of Well-defined PAA-PEG Multi-responsive Hydrogels by ATRP and Click Chemistry

Author: Chao Zhou, Shan-shan Qian, Xia-jun Li, Fang Yao, John S. Forsythe* and Guo-dong Fu*

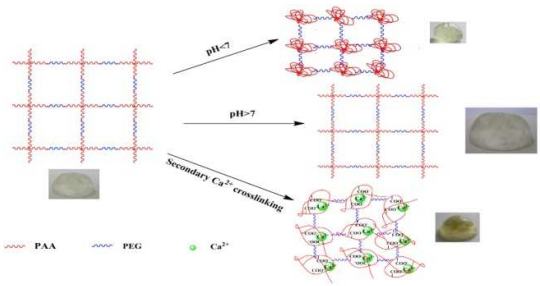

Well-defined multi-responsive PAA-PEG hydrogel exhibit a unique swelling property at different pH and Ca^{2+} secondary crosslinking, and can potentially be used as a stimuli responsive biomaterial.